European Review for Medical and Pharmacological Sciences 2019; 23: 8274-8286

Characterization of hsa_circ_0000594 as a new biomarker and therapeutic target for hepatoblastoma

H. SONG[1], Z.-X. BIAN[1], H.-Y. LI[1], Y. ZHANG[2], J. MA[1], S.-H. CHEN[3], J.-B. ZHU[1], X. ZHANG[1], J. WANG[4], S. GU[4], M. XU[4], Q.-H. PAN[1], M.-Z. YIN[5], L. ZHENG[6]

[1]Department of Laboratory Medicine, Shanghai Children's Medical Center, School of Medicine, Shanghai Jiaotong University, Shanghai, China
[2]Department of Central Laboratory, Shanghai Tenth People's Hospital, Tongji University, Shanghai, China
[3]Department of Laboratory Medicine, Yunfu People's Hospital, Guangdong, China
[4]Department of Surgery, Shanghai Children's Medical Center, School of Medicine, Shanghai Jiaotong University, Shanghai, China
[5]Department of Pathology, Shanghai Children's Medical Center, School of Medicine, Shanghai Jiaotong University, Shanghai, China
[6]Pediatric Translational Medicine Institute, School of Medicine, Shanghai Jiaotong University, Shanghai, China

Hang Song, Zhixuan Bian, Huaiyuan Li are contributed equally to this work

Abstract. – OBJECTIVE: Various studies have shown that aberrant expression of circular RNAs (circRNAs) has a pivotal role in multifarious cancers. However, the role of circRNAs in hepatoblastoma (HB) is not clearly understood. In the present study, we attempted to explore the underlying mechanism of hsa_cric_0000594 in HB along with its clinical importance.

PATIENTS AND METHODS: In our research, the expression pattern of hsa_circ_0000594 in HB tissues and matched normal liver tissues was determined by in situ hybridization and RT-qPCR. Proliferation, viability, migration, and apoptosis of HB cell lines were detected *via* Cell Counting Kit-8 (CCK-8), colony formation, transwell, and flow cytometry assays. The interaction of hsa_circ_0000594 with miR-217 was investigated by Dual-Luciferase reporter assay.

RESULTS: Expression levels of hsa_circ_0000594 were significantly upregulated in HB tissues compared with those in paired normal liver tissues and showed a clear association with the subtype of HB. The knockdown of hsa_circ_0000594 inhibited the malignant phenotype of HB. Bioinformatics analysis suggests that sirtuin 1 (SIRT1) may serve as a target gene of miR-217.

CONCLUSIONS: Mechanically, hsa_circ_0000594 was identified to have a critical role in HB development through the hsa_circ_0000594/mir-217/SIRT1 regulatory axis, which might become a novel diagnostic marker and potential therapeutic target in HB.

Key Words:
Circular RNA, Hsa_circ_0000594, Hepatoblastoma, MiR-217, SIRT1.

Introduction

Hepatoblastoma (HB) is a common type of primary malignant hepatic tumor usually identified in children during the first 3 years of life. The annual incidence rate of HB is extremely low at 1.5 per million of population. The exact mechanism of this cancer is unknown but it is assumed to originate from abnormal stem cells and early hepatic epithelial progenitor cells[1]. Despite its low occurrence, the Surveillance, Epidemiology, and End Results (SEER) program of the National Cancer Institute in the US has reported that HB accounts for almost 79% of pediatric liver cancers. This pediatric cancer has received considerable critical attention due

Corresponding Authors: Qiuhui Pan, MD; e-mail: panqiuhui@scmc.com.cn
Minzhi Yin, MD; e-mail: yinminzhi@scmc.com.cn
Liang Zheng, MD; e-mail: Zhengliangscmc@sina.com

to its dreadful prognosis resulting from the ambiguous incipient symptoms and high frequency of metastasis and recurrence[2]. The 5-year survival rate of children with HB is over 70% due to treatment regimens involving systemic chemotherapy and surgical resection[1]. However, given the increasing incidence of HB, there is an ongoing need to deliver new reliable diagnostic methods and markers besides alpha fetoprotein (AFP)[3] and β-catenin[4] to support prompt diagnosis and optimum treatment, as well as to improve the precision of prognosis. Hence, the discovery of novel biomarkers to improve diagnosis and treatment, especially during the initial stages of HB, is urgently required.

Circular RNAs (circRNAs), a novel class of endogenous RNAs expressed in all types of organisms, are formed by back-splicing events and characterized by covalently closed continuous loops without a 5' cap or a 3' poly(A) tail. Qu et al[5] suggest that circRNAs usually exhibit tissue/developmental-stage-specific expression and may be engaged in the initiation and development of various diseases such as neurological disorders, cancer, atherosclerosis, and prion-related diseases. It is now well established that circRNAs have been observed to be abnormally expressed in various cancer types and have an important role in the carcinogenesis and progression of cancer. For instance, Hansen et al[6] demonstrated that ciRS-7, originating from the CDR1 gene and one of the best studied circRNAs, has more than 70 miRNA binding sites. This circRNA serves as a miRNA sponge to silence the expression of miRNA-7 and its downstream targeted genes, which can promote the proliferation, invasion, and metastasis of cancer cells.

Several studies have postulated that circRNAs can be novel promising molecular biomarkers in a range of cancers. CircRNAs are a group of highly conserved and tissue-specific RNA molecules by virtue of their distinct circular covalently closed structure and specific expression pattern, and lack 5' or 3' polarity, leading to stronger tolerance to RNase R, as well as having better stability than linear RNAs, which cannot resist digestion by RNase R[7-10]. Two circRNAs, hsa_circRNA_100855 and hsa_circRNA_104912, were reported to be significantly upregulated and downregulated in laryngeal squamous cell cancer tissues (LSCC), respectively, when compared with adjacent non-tumor tissues[11]. Their expression was closely associated with neck nodal metastasis, differentiation degree, and advanced clinical stage of patients, supporting their potential as novel biomarkers for the diagnosis and progression of LSCC. Liu et al[12] suggested that circRNAs are involved in the pathogenesis of HB and that circ_0015756 is a promising target for the diagnosis, prognosis, and management of HB. Nevertheless, there is still no systematic understanding of how circRNAs contribute to HB.

In this study, we first analyzed the expression patterns of hsa_circ_0000594 in HB tissues and matched non-tumor liver tissues using qRT-PCR and *in situ* hybridization. The results demonstrated that its expression level was significantly upregulated in HB tissues. Additionally, we found that hsa_circ_0000594 could influence the development and progression of HB by directly regulating the miR-217/SIRT1 pathway. These results provide adequate evidence that hsa_circ_0000594 has a critical role in HB and may act as a diagnostic marker and therapeutic target in HB.

Patients and Methods

Tissue Specimens and HB Cell Lines

Twenty-four pairs of human HB and matched non-tumor liver tissues were collected from patients undergoing hepatectomy surgery at the Department of Hepatobiliary Surgery of Shanghai Children's Medical Center (Shanghai, China). Detailed clinicopathological information of each HB tissue sample was available. These patients had not received chemotherapy, radiotherapy, or targeted therapy before admission. This investigation was approved by the Ethics Committee of Shanghai Children's Medical Center and informed consent was obtained from each patient.

HB cell lines HepG2 and Huh6 obtained from the Cell Bank of the Chinese Academy of Sciences (Shanghai, China) were cultured in Minimum Eagle's Medium (MEM) and Dulbecco's Modified Eagle's Medium (DMEM), respectively, supplemented with high glucose, 10% fetal bovine serum (FBS), 100 μg/ml streptomycin, and 100 U/ml penicillin in 5% CO_2 at 37°C.

In Situ Hybridization and Immunohistochemistry

The expression level of hsa_circ_0000594 in tissues was assessed by *in situ* hybridization (ISH) according to a previous protocol[13]. Briefly,

Table I. Sequence of ISH probes.

Probe	Sequence (5′-3′)
Hsa_circ_0000594	CAATCTTTCTCAATGGTCTGACGTCA
Negative Control (NC)	GTGTAACACGTCTATACGCCCA

ISH was performed on 5-μm-thick tissue sections from HB tissues and matched normal tissues (n=24). After pretreatment, tissue sections were hybridized overnight with digoxygenin (DIG)-labeled probes specific for hsa_circ_0000594. Then, slides were incubated with anti-DIG-HRP antibody (#ab6212; Abcam, Cambridge, MA, USA) at room temperature for 1 h, and the specific hybridization reaction of the DIG-linked probes was observed using diaminobenzidine (DAB) substrate. To visualize the complete morphology of tissues, the slides were counterstained with hematoxylin and subsequently examined under a bright-field microscope. The probe sequences are listed in Table I.

The protein levels of β-catenin and glypican-3 in tissues were examined by immunohistochemistry (IHC). Briefly, tissue sections from HB tissues and matched normal tissues (n=24) were routinely dewaxed and rehydrated. After antigen retrieval and blocking of endogenous peroxidase and non-specific binding, sections were incubated with primary antibody against β-catenin (#ab22656; Abcam, Cambridge, MA, USA) and glypican-3 (#ab129381; Abcam, Cambridge, MA, USA), followed by incubation with biotinylated secondary anti-mouse IgG antibody (#ab6789; Abcam, Cambridge, MA, USA), and horseradish peroxidase (HRP)-labeled streptavidin antigen was visualized after incubation with DAB. Representative images were photographed under a microscope (Leica, Buffalo Grove, IL, USA).

RNA Isolation and Real Time-Quantitative Reverse-Transcription Polymerase Chain Reaction (RT-qPCR)

Total RNA from HB tissues and cell lines was extracted using TRIzol reagent (Invitrogen, Carlsbad, CA, USA) in accordance with the manufacturer's protocol. One microgram of total RNA was utilized to synthesize cDNA with the PrimeScript™ RT Reagent Kit (TaKaRa, Dalian, Liaoning, China). RT-qPCR was performed with KAPA SYBR® FAST qPCR Kit Master Mix (2X) Universal (Applied Biosystems, Foster City, CA, USA) on an ABI7900 Real-Time PCR Detection System (Applied Biosystems, Foster City, CA, USA). All data were analyzed by the $2^{-\Delta\Delta CT}$ method. Primers used are listed in Table II.

Oligonucleotides and Transfection

SiRNAs for hsa_circ_0000594, siRNA-NC, miR-217 mimics, miR-NC mimics, miR-217 inhibitor, and miR-NC inhibitor were chemically synthesized by GenePharma (Shanghai, China). All transfections were conducted using Lipofectamine 2000 transfection reagent (Invitrogen, Carlsbad, CA, USA) in accordance with the manufacturer's instructions.

Table II. Sequence of primers.

Primer	Sequence (5′-3′)
Hsa_circ_0000594	F: GCTTGGCTCGACAATTTACC R: AGTGCAACATTTTCCCTGGT
GAPDH	F: AAATCCCATCACCATCTTCCAG R: TGATGACCCTTTTGGCTCCC
SIRT1	F: GTATTTATGCTCGCCTTGCTG R: TGACAGAGAGATGGCTGGAA RT: CATGATCAGCTGGGCCAAGAATCCAGTGAGTT
miR-217	F: TACTGCATCAGGAACTGACTGGA R: TACTGCATCAGGAACT RT: AAAAATATGGAACGCTCACGAATTTG
U6	F: GTGCTCGCTTCGGCAGCACATATAC R: AAAAATATGGAACGCTCACGAATTTG

Cell Proliferation and Colony Formation Assays

For cell counting kit-8 (CCK-8) assays, cells were seeded into 96-well plates at a density of 5,000 cells per well in triplicate. After treatment, the cells were cultured in 100 µl of fresh medium, which was supplemented with 10 µl of CCK-8 reagent (Beyotime, Shanghai, China) and incubated at 37°C for 3 h. Finally, the absorbance was determined at a wavelength of 450 nm by a multiplate reader (Bio Tek, Winooski, VT, USA).

For colony formation assays, cells were seeded into 12-well plates at a density of 1,000 cells per well. The cells in the plates were incubated for approximately 7 days in fresh medium and stained with 0.1% crystal violet. The numbers of cell colonies represented the colony-forming ability.

Cell Apoptosis Analysis

HB cells transfected with siRNA-hsa_circ_0000594_1 or negative control were collected followed by washing with pre-chilled phosphate-buffered saline (PBS). Next, 5×10^5 cells were treated with 50 µl of Annexin V-Binding buffer comprising 2.5 µl of Annexin-V-FITC. After incubation, propidium iodide (PI) was added in the dark to stain necrotic cells. Finally, fluorescence-activated cell sorting (FACS) analysis was performed using BD FACSCanto II™ (Franklin Lakes, NJ, USA) to evaluate the percentage of apoptotic cells.

Cell Migration Assay

Cell invasion ability was evaluated by transwell assays. In brief, cells (approximately 4×10^4) were collected at 48 h after transfection, followed by resuspension in serum-free medium and seeding in the upper chamber of a transwell plate, with normal culture medium added to the lower chamber. After 24 h of incubation at 37°C with 5% CO_2, the cells migrating through the membrane were fixed by polyoxymethylene and then stained with 0.1% crystal violet.

Dual-Luciferase Reporter Assay

The full-length sequence of hsa_circ_0000594 containing the binding site of miR-217 and mutant hsa_circ_0000594 were cloned downstream of the *Renilla* luciferase gene of Dual-Luciferase plasmid pGL4.21 vector (Promega, Madison, WI, USA) to construct the pGL4.21-hsa_circ_0000594 vector or pGL4.21-hsa_circ_0000594-Mut vector. Afterwards pGL4.21-hsa_circ_0000594 vector or pGL4.21-hsa_circ_0000594-Mut vector together with miR-217 mimics or negative control mimics were co-transfected into HB cell lines HepG-2 and Huh6 using Lipofectamine 2000 (Invitrogen, Carlsbad, CA, USA). Forty-eight hours later, firefly and *Renilla* signals were detected using a Dual-Luciferase system (E1910; Promega, Madison, WI, USA).

Bioinformatics Analysis

Three circRNA-related databases, CircInteractome (https://omictools.com/circinteractome-tool), starBase (http://starbase.sysu.edu.cn/), and CircBank (http://www.circbank.cn/), along with three miRNA-related databases, TargetScan (http://www.targetscan.org/vert_72/), miRDB (http://mirdb.org/), and miRPathDB (https://mpd.bioinf.uni-sb.de/), were used to track the underlying target miRNAs of hsa_circ_0000594 and the potential target genes of miR-217. The predicted target genes of miR-217 were inputted into DAVID (http://david.abcc.ncifcrf.gov) for gene annotation and functional analysis, comprising Gene Ontology (GO) and KEGG pathway analysis. The protein-protein interaction (PPI) network was analyzed by the STRING database (https://string-db.org/) and illustrated by Cytoscape (https://cytoscape.org/).

Western Blotting Assay

Total protein was extracted in RIPA lysis buffer (Beyotime, Shanghai, China), quantified, and boiled in sodium dodecyl sulphate (SDS). Afterwards, 60 µg of protein was separated by 10% sodium dodecyl sulphate-polyacrylamide gel electrophoresis (SDS-PAGE) and then transferred to nitrocellulose membranes (GE Healthcare, Natick, MA, USA). The membranes were blocked with 5% bovine serum albumin (BSA) and subsequently incubated for 1 h at 37°C with primary antibody against SIRT1 (#ab110304; Abcam, Cambridge, MA, USA) and GAPDH (#ab9484; Abcam, Cambridge, MA, USA). After washing, membranes were incubated with fluorescent-conjugated secondary antibodies (LI-COR Biosciences, Lincoln, NE, USA) for 1 h at room temperature. Finally, the bands on the membranes were visualized using an Odyssey instrument (LI-COR Biosciences, Lincoln, NE, USA). Glyceraldehyde-3-phosphate dehydrogenase (GAPDH) was used as an internal control.

Statistical Analysis

All experiments were repeated at least three times. Pearson's correlation coefficient was utilized to analyse the correlations between two parameters. Data were analyzed using one-way ANOVA with the Scheffé post-hoc test. Data are presented as the mean ± standard deviation (SD). The statistical significance is indicated as $*p<0.05$ and $**p<0.01$.

Results

Hsa_circ_0000594 Is Upregulated in HB Specimens, Primarily in Epithelium

ISH was performed on 24 pair of HB tissue specimens and matched non-tumor liver tissues to examine the transcriptional expression levels of hsa_circ_0000594. ISH generated distinct and positive DIG-labeled hybridization signals for hsa_circ_0000594 in the tissue specimens. The results of ISH revealed that the intensity and extent of hybridization signals for hsa_circ_0000594 in HB tissues were significantly higher than those in paired non-tumor liver tissues, particularly in epithelial tissues, which proved that hsa_circ_0000594 expression in HB tissues was significantly upregulated compared with that in normal liver tissues, and that hsa_circ_0000594 was mainly expressed in epithelial rather than mesenchymal tissues (Figure 1A). Zhou et al[14] identified that HB epithelium has a distinct immunohistochemical profile with glypican-3 and β-catenin, which might promote the differentiation of diverse HB subtypes and distinguishing HB from HCC. Consequently, we attempted to detect whether hsa_circ_0000594 could serve as a marker of HB like glypican 3 and β-catenin. IHC and ISH were performed to detect the expression of glypican 3, β-catenin, and hsa_circ_0000594 in HB tissues and matched normal liver tissues. As shown in Figure 1B, hsa_circ_0000594 shared the same expression pattern as glypican-3 and β-catenin in that hsa_circ_0000594 was highly expressed in the cytoplasm but not in the nuclei of HB epithelial cells, which suggested that hsa_circ_0000594 could be a latent molecular biomarker for HB diagnosis. Moreover, the RT-qPCR results, which were normalized to 18s rRNA, revealed the relative transcriptional expression levels of hsa_circ_0000594 in each specimen of HB tissue and matched non-tumor liver tissue, further verifying our observations from ISH (n=24; $**p<0.01$) (Figure 1C).

Hsa_circ_0000594 Is Required for HB Malignant Phenotypes

To confirm whether hsa_circ_0000594 stimulates transformed phenotypes in HB cells, two independent short interfering RNAs (siRNAs) targeting hsa_circ_0000594 were introduced and the transfection efficiency was validated by qRT-PCR. As expected, hsa_circ_0000594 siRNA transfection significantly reduced hsa_circ_0000594 expression in HepG2 and Huh6 cells (Figure 2A). We selected hsa_circ_0000594-siRNA-1 with better silencing efficiency for the subsequent studies. CCK8 assays (Figure 2B) and colony formation assays (Figure 2C) demonstrated that hsa_circ_0000594 silencing remarkably reduced the proliferation and viability of HB cells. In addition, by knocking down hsa_circ_0000594 in HepG2 and Huh6 cells, a significant reduction in cell migration capacity was observed (Figure 2D). Moreover, we observed that silencing of hsa_circ_0000594 induced total apoptosis in HepG2 and Huh6 cells, which could be analyzed through FACS. In general, therefore, hsa_circ_0000594 is required to maintain the malignant phenotype in HB cells.

Hsa_circ_0000594 Serves as a Sponge for MiR-217 and MiR-217 Is Required for Hsa_circ_0000594 to Exert its Effects in HB

It has been conclusively shown that circRNAs can function as miRNA sponges[15] and our previous studies found that hsa_circ_0000594 was abundant in the cytoplasm, suggesting that hsa_circ_0000594 may regulate HB cells by sponging miRNAs. Three powerful web tools, CircInteractome, starBase, and CircBank, were exploited to predict the underlying binding miRNAs of hsa_circ_0000594. Strikingly, only one miRNA, miR-217, was identified in all three independent databases (Figure 3A); the potential binding site between hsa_circ_0000594 and miR-217 is presented in Figure 3B. The expression level of miR-217 was investigated by RT-qPCR, showing that miR-217 was prominently downregulated in HB tissues compared with that in matched non-tumor liver tissues (Figure 3C). Furthermore, the expression level of miR-217 in HB cell lines was reduced upon the silencing of hsa_circ_0000594 (Figure 3D). To validate whether miR-217 could directly target hsa_circ_0000594, we performed Dual-Luciferase assays. Hsa_circ_0000594 or mutant hsa_circ_0000594 cDNA (shown in Figure 3B) cloned downstream of the luciferase gene

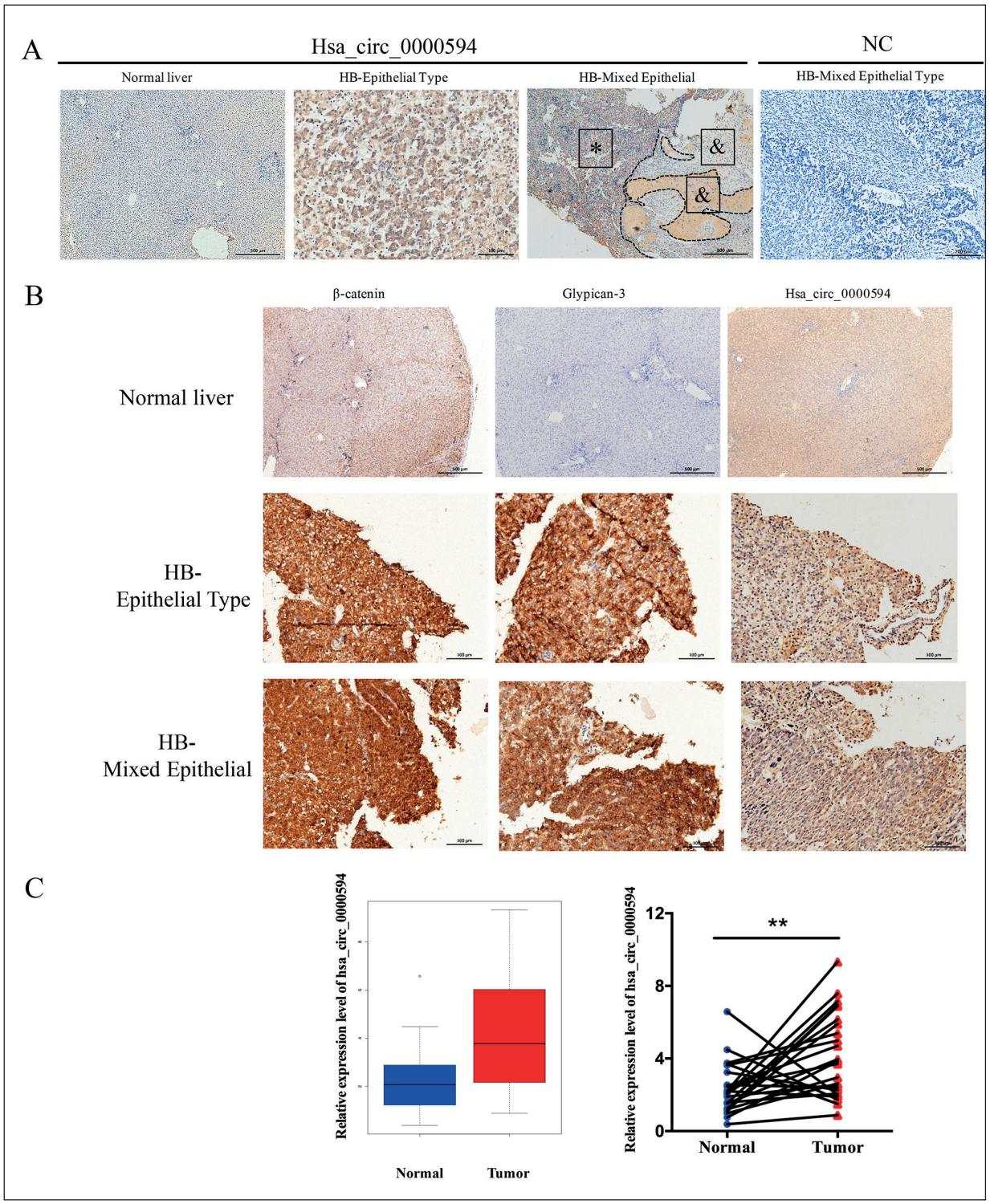

Figure 1. Hsa_circ_0000594 is upregulated in HB tissues and identical to glypican-3 and β-catenin in terms of sharing the same expression pattern. **A**, ISH was utilized to evaluate the expression level of hsa_circ_0000594 in HB tissues and matched normal liver tissues (n=24). *Represents epithelial tissues and & represents mesenchymal tissues (200×). **B**, ISH and IHC were used to detect the expression pattern of hsa_circ_0000594, glypican 3, and β-catenin in HB tissues using serial sections (n = 24). Representative images are shown (200×). **C**, Transcriptional expression levels of hsa_circ_0000594 in paired HB and normal liver tissues were analyzed by RT-qPCR. $^{**}p < 0.01$.

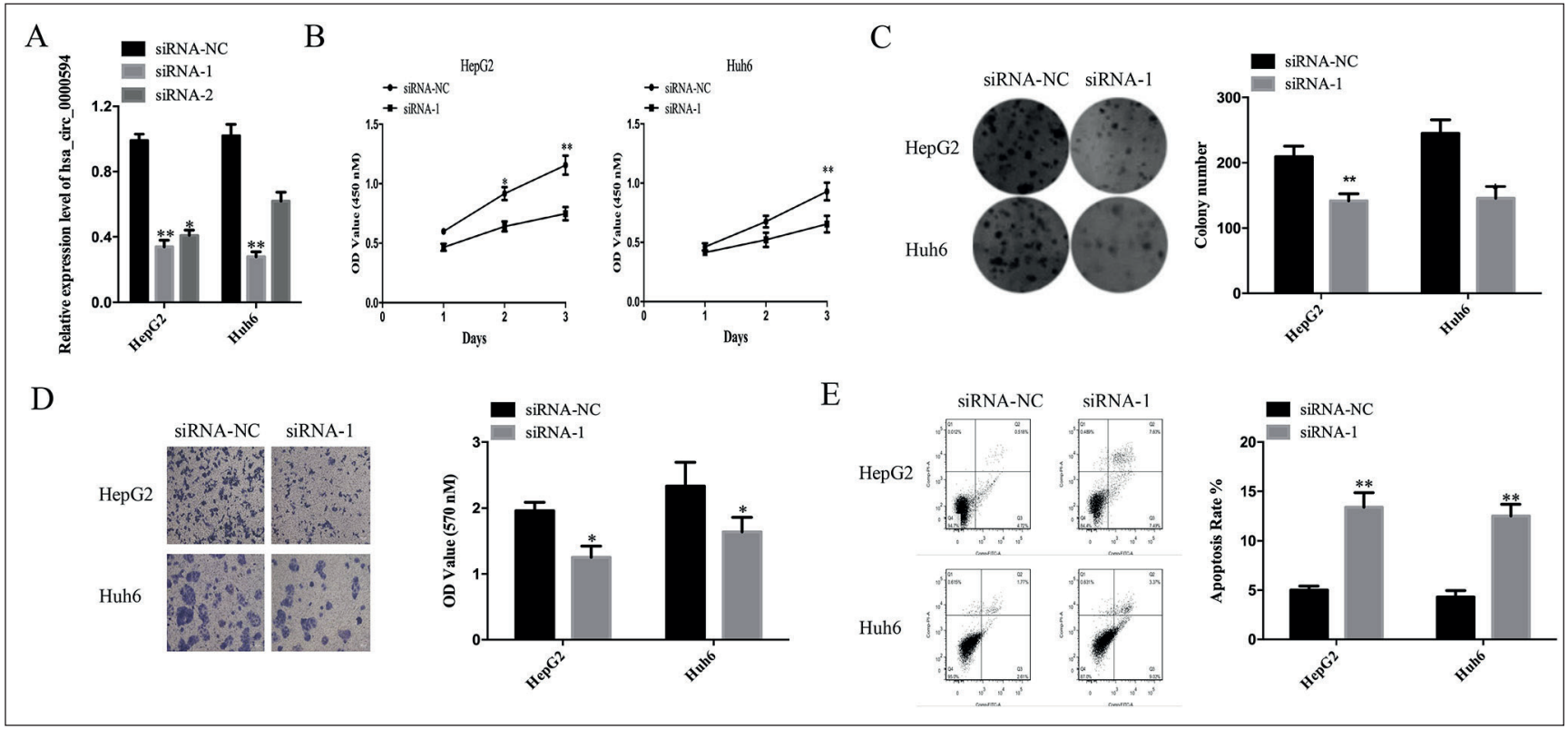

Figure 2. Hsa_circ_0000594 is required to maintain the malignancy of HB. **A**, Expression of hsa_circ_0000594 under the indicated conditions was measured by RT-qPCR. Proliferation, viability, invasion ability and apoptosis in treated HB cell were detected by CCK8 assays (**B**), colony formation assays (**C**, magnification 100×), transwell assays (**D**, magnification 200×) and FACS analysis (**E**), respectively. *p<0.05, **p<0.01.

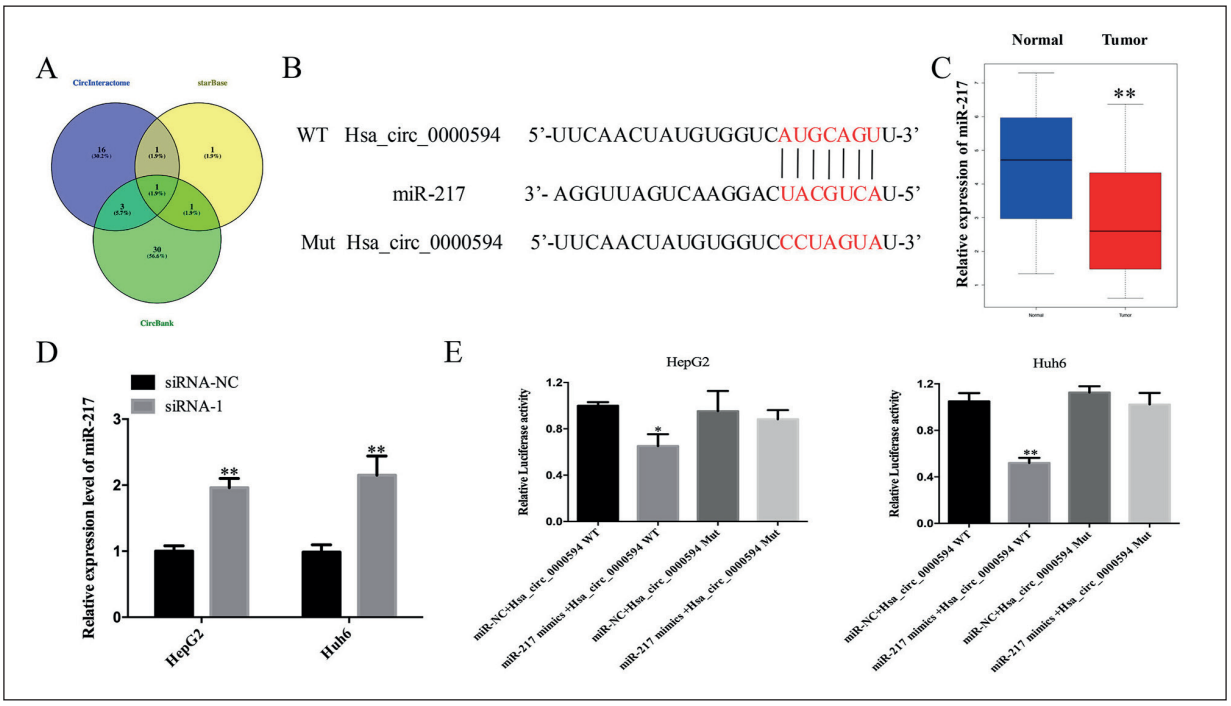

Figure 3. Hsa_circ_0000594 serves as a sponge for miR-217. **A**, Venn diagram showing the putative target miRNAs of hsa_circ_0000594 in three independent databases. **B**, The potential binding sites of miR-217 on hsa_circ_0000594. **C**, Expression level of miR-217 in paired HB tissues and normal liver tissues was determined by RT-qPCR. **D**, The expression level of miR-217 in hsa_circ_0000594 silencing HB cell lines. **E**, Dual-Luciferase assays confirmed the interaction of hsa_circ_0000594 with miR-217. **p*<0.05, ***p*<0.01.

and miR-217 mimics or negative control mimics (miR-NC) were serially co-transfected into HepG2 and Huh6 cells. The results indicated that miR-217 significantly inhibited the luciferase reporter activity of hsa_circ_0000594 and had no effect on hsa_circ_0000594-Mut activity, suggesting that hsa_circ_0000594 could bind to miR-217 and the binding site was just as predicted (Figure 3E). Notably, hsa_circ_0000594-siRNA-1-mediated inhibition of the transformed phenotypes could be reversed by simultaneous co-expression of miR-217 inhibitor (Figure 4A-4C). The above results suggest that hsa_circ_0000594 serves as a sponge for miR-217 to improve proliferation and invasion and reduced the apoptosis of HB cells.

Hsa_circ_0000594 Regulates the Expression of MiR-217 Target Gene, SIRT1, in HB Cells

Three bioinformatic tools, namely TargetScan, miRDB, and miRPathDB, were employed to predict the underlying targets of miR-217, and 137 genes were intersected in a Venn diagram (Figure 5A). The predicted 137 target genes of miR-217 were inputted into DAVID for gene annotation and a functional analysis comprising Gene Ontology (GO) and Kyoto Encyclopedia of Genes and Genomes (KEGG) pathway analyses. Genes annotated with GO terms were identified to be expressed mostly in the cytoplasm and to be specific to protein binding (Figure 5B, C). As shown in Figure 5D, the 137 target genes of miR-217 mainly participated in the class O of forkhead box transcription factor (FOXO) signaling pathway, endometrial cancer, glutamatergic synapse, non-small cell lung cancer, acute myeloid leukemia, and renal cell carcinoma, indicating that these genes might have functions in several cancer types. Moreover, the protein-protein interaction network (PPI network) was analyzed by STRING and illustrated by Cytoscape (Figure 5E). This network suggested that SIRT1 acted as a hub linking other protein nodes. NAD-dependent protein deacetylase sirtuin-1 (SIRT1), an oncoprotein found in many cancers including B-cell lymphoma[16], ovarian cancer[17], breast cancer[18], and hepatocellular carcinoma (HCC)[19], may be a feasible target gene of miR-217. QPCR and western blotting analyses revealed that increased levels of miR-217 could inhibit the expression of SIRT1 in HB cell lines (Figure 5F, 5G). More importantly, we found that the expression levels of

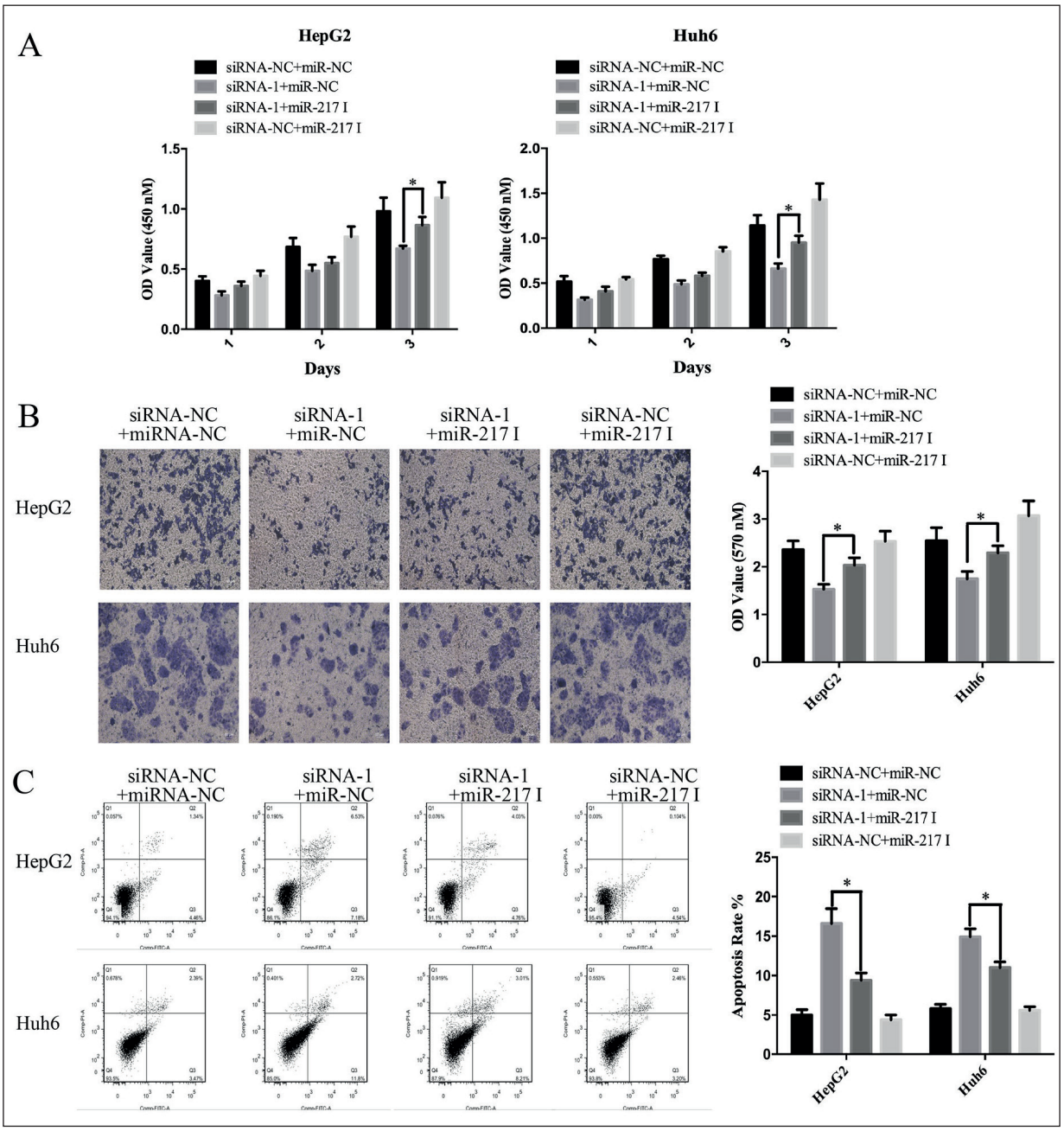

Figure 4. MiR-217 is required for hsa_circ_0000594 to exert effects in HB. Hsa_circ_0000594-siRNA-1-mediated inhibition of the transformed phenotypes was reversed by co-expression of miR-217 inhibitor. Levels of cell proliferation, apoptosis, and invasion ability were measured by CCK8 (**A**), transwell assay (**B**, magnification 200×), and FACS analysis (**C**), respectively. *$p<0.05$, **$p<0.01$.

SIRT1 were negatively correlated with miR-217 in HB tissues (Figure 5H), suggesting that SIRT1 could serve as a direct target of miR-217 in HB. Collectively, these results demonstrated that the hsa_circ_0000594/miR-217/SIRT1 axis may have critical roles in the progression and development of HB (Figure 6).

Discussion

In this study, we first verified that hsa_circ_0000594, which was derived from the oncogenic tau tubulin kinase 2 (TTBK2) gene[20], naturally exists as a loop in HB tissues. Meanwhile, the expression levels of hsa_circ_0000594

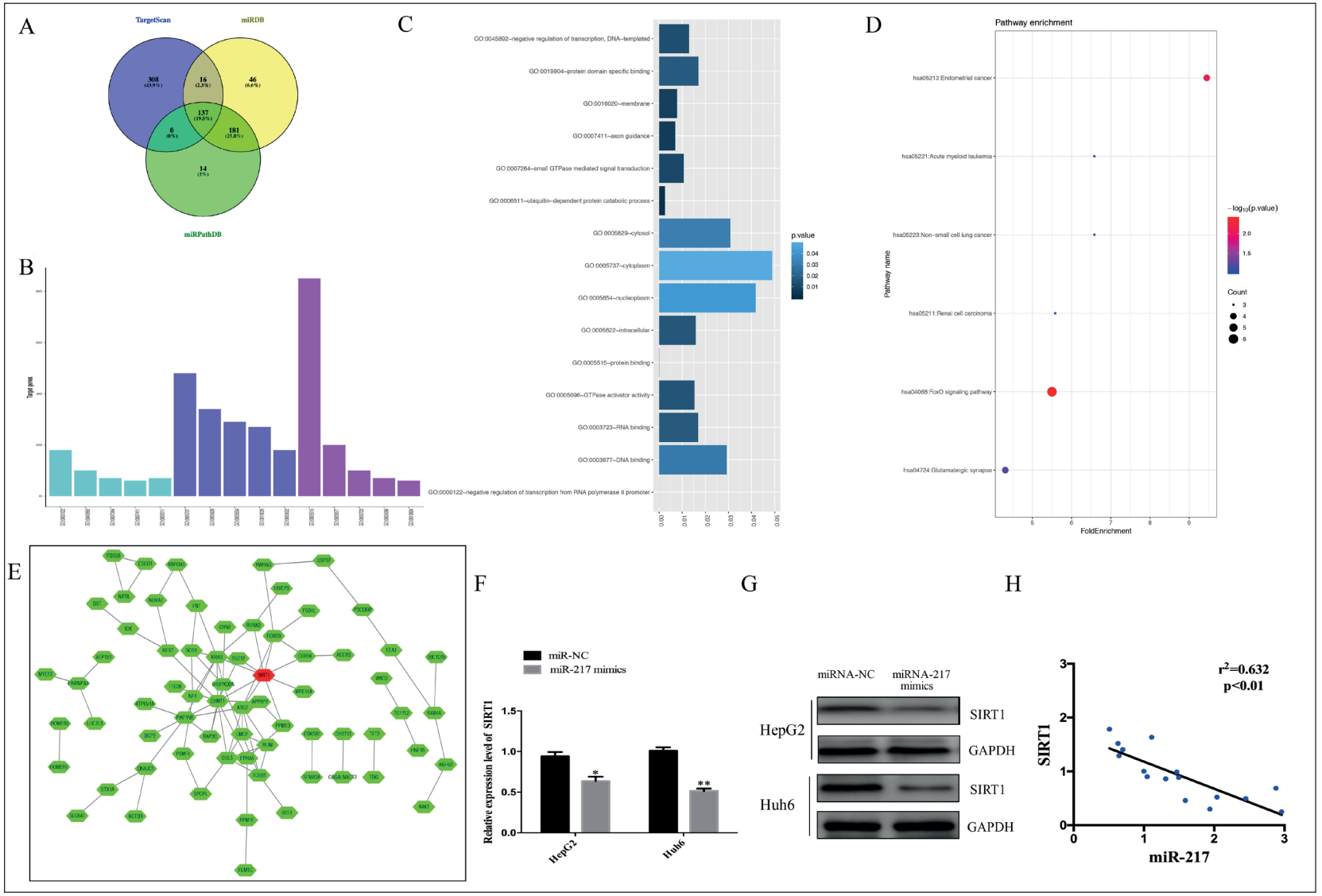

Figure 5. Hsa_circ_0000594 regulates the expression of miR-217 target gene, SIRT1, in HB cells. **A**, Venn diagram showing the putative target genes of miR-217 in three independent databases. GO (**B, C**), and KEGG pathway analysis (**D**) were carried out by DAVID. (**E**) PPI network of SIRT1 was established by STRING and Cytospace. (**F, G**) The expression levels of SIRT1 were analyzed by RT-qPCR and Western blot. (**H**) Correlation between miR-217 and SIRT1 was detected by RT-qPCR. *$p<0.05$, **$p<0.01$.

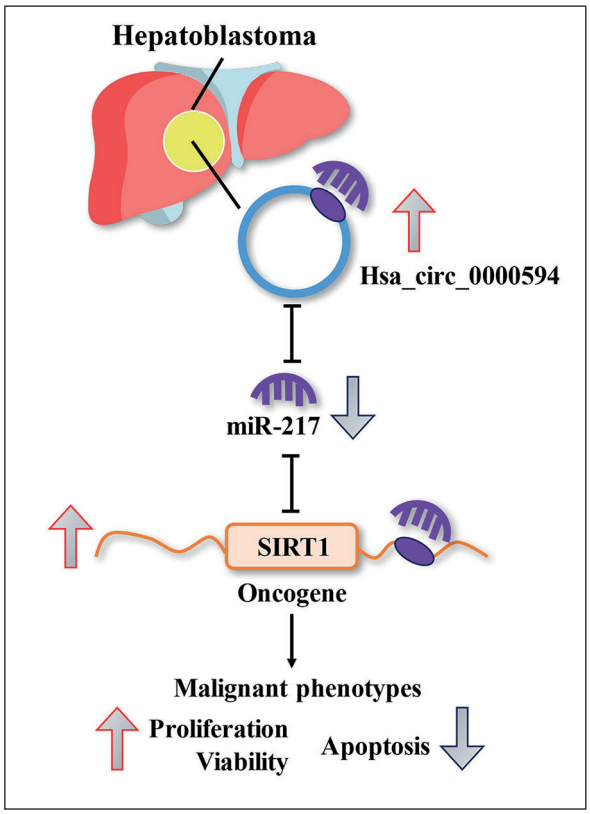

Figure 6. Schematic of the hsa_circ_0000594/miR-217/SIRT1 axis in HB.

were markedly upregulated in HB tissues when compared with those in matched non-tumor liver tissues. Results from CCK8, colony formation, and transwell assays and FACS analysis demonstrated that hsa_circ_0000594 in HB improved cell proliferation, viability, and invasion capacity and reduce apoptosis, suggesting its potential role in tumor growth and migration. Although the underlying mechanisms of hsa_circ_0000594 and its binding miRNA miR-217 in HB remained to be further studied, hsa_circ_0000594 clearly has the potential to serve as a novel biomarker for HB diagnosis.

HB is a rather malignant embryonal hepatic neoplasm that mainly occurs in infants and children under the age of 15, accounting for approximately 1% of pediatric cancers[1]. Considering that HB is the most common primary liver tumor and the third most common abdominal tumor in childhood, along with its increasing incidence[21], it holds great clinical significance and value. Most HB patients have a poor prognosis since it is difficult to make an early diagnosis due to the ambiguous and nonspecific incipient symptoms resulting from the pathological characteristics of HB and its heterogenous histological subtypes[2]. In addition, distant metastases often occur in roughly 20% of patients with HB at the time of diagnosis[22]. Consequently, the key to improving the prognosis of HB patients relies on early detection and timely treatment. At present, serum AFP is the most prominent diagnostic biomarker for HB because it is markedly elevated in almost 90% of patients with the disease[23]. In addition, previous studies have reported that AFP is the only prognostic marker used in a clinical context to monitor therapeutic response and survey recurrence after treatment. A low level (<100 ng/ml) of serum AFP and an extremely high level of serum AFP (>1.2×10^6 ng/ml) at HB diagnosis are predictors of a poor prognosis[24]. The prognostic roles of other molecules have been evaluated in HB. For instance, the co-expression of nuclear β-catenin and membranous epithelial cell adhesion molecule (EpCAM) in HB tissue specimens was found to be significantly linked to a drop in serum AFP level (< 1200 ng/mL) after neoadjuvant chemotherapy, which implied better chemosensitivity[25]. In addition, glypican-3 and β-catenin were suggested to help differentiate diverse HB subtypes and distinguish HB from HCC due to their distinct immunohistochemical profile in HB epithelium[14]. However, given that the serum level of AFP may also be increased in patients with benign liver neoplasms such as hemangioendotheliomas, hepatic adenoma, and mesenchymal hamartoma, and in patients with HCC[26], and that it is naturally high in infants, AFP is not an ideal and specific biomarker for the diagnosis and prognosis of HB. Thus, there is an urgent need to develop novel and effective biomarkers.

With the development of advanced technologies and bioinformatics, circRNAs have received increasing attention. Qin et al[27] revealed that the expression of hsa_circ_0001649 was significantly decreased in HCC tissues when compared with that in paired adjacent non-tumor liver tissues, and the receiver operating characteristics (ROC) analysis for hsa_circ_0001649 in HCC showed its great potential as a diagnostic biomarker of HCC with high sensitivity, specificity, and accuracy. Similarly, hsa_circ_0000190 expression was reported to be markedly downregulated in plasma specimens and gastric cancer (GC) tissues from GC patients, and displayed significant correlations with TNM stage, tumor diameter, lymphatic and distal metastasis, and CA19-9 and CEA levels, supporting it as a non-invasive biomarker for the auxiliary diagnosis of GC[28]. However, few

studies have examined the association between circRNAs and HB. Our results from RT-qPCR and ISH revealed that in contrast to the paired normal liver tissues, the expression level of hsa_circ_0000594 was significantly upregulated in tissue specimens from patients with HB, and that the expression pattern of hsa_circ_0000594 coincided with that of glypican-3 and β-catenin, indicating the possibility of using hsa_circ_0000594 as a more effective and specific biomarker than AFP for the diagnosis of HB.

MiRNAs are a class of endogenous small non-coding RNAs (18-25 nucleotides) that suppress ribosome function and promote the degradation of target mRNAs to regulate gene expression at the post-transcriptional level via binding to specific sites on the 3'-UTRs of target genes[29]. MiR-217 has been documented to be involved in carcinogenesis and tumor development in several cancers, such as glioblastoma[30], breast cancer[31], and HCC[32]. In this study, we explored whether miR-217 is an important target of hsa_circ_0000594 in HB cells through bioinformatics analysis. Individual knockdown of hsa_circ_0000594 in HB cells resulted in decreased proliferation, viability, and invasion ability and increased apoptosis, which could be significantly reversed upon the simultaneous co-transfection with miR-217 inhibitor. However, miR-217 inhibitor alone had no effect, probably due to the initial low expression of miR-217 in HB tissues. In addition, three miRNA-related databases were applied to search for target genes of miR-217, identifying SIRT1. QPCR and Western blot analysis demonstrated a negative correlation between miR-217 and SIRT1. The observations led to the consensus that hsa_circ_0000594 exerted its pivotal function in maintaining the transformed phenotypes of HB via sponging miR-217, a well-recognized tumor suppressor miRNA, to regulate SIRT1 expression.

Conclusions

Taking the findings of this study together, we first identified that hsa_circ_0000594 expression was significantly upregulated in HB tissues, thereby distinguishing cancerous from non-cancerous tissues. Owing to the limitation of the relatively small sample size in this study, there was insufficient statistical power to validate any associations; for instance, the correlation between the expression pattern of hsa_circ_0000594 and the histological subtypes of HB. Nevertheless, we did reveal that hsa_circ_0000594 might serve as a promising diagnostic and prognostic biomarker for HB patients. Future discoveries hinge on a large-scale study to elucidate the significant relationships among cell markers, histological subtypes, and the survival of patients with HB. Furthermore, our results established that hsa_circ_0000594 is involved in the tumorigenesis and metastasis of HB, indicating that the blocking of hsa_circ_0000594 might be a promising therapeutic strategy for treating HB.

Conflict of Interest

The Authors declare that they have no conflict of interests.

Acknowledgements and Funding

We thank all of the staff at the Department of Laboratory Medicine of Shanghai Children's Medical Center affiliated to Shanghai Jiaotong University School of Medicine. We also thank Liwen Bianji, Edanz Group China (www.liwenbianji.cn/ac), for editing the English text of a draft of this manuscript. This investigation was financially supported by the National Natural Science Foundation of China (81572330, 81802103, 81772941, 81702741 and 81871727), a Municipal Human Resources Development Program for Outstanding Leaders in Medical Disciplines in Shanghai (2017BR036), Program of Shanghai Academic/Technology Research Leader (18XD1402600), Shanghai Municipal Education Commission-Gaofeng Clinical Medicine Grant Support (20171926) and Science and Technology Development Fund of Pudong New Area of Shanghai (PKJ2017-Y03).

References

1) Allan BJ, Parikh PP, Diaz S, Perez EA, Neville HL, Sola JE. Predictors of survival and incidence of hepatoblastoma in the paediatric population. HPB (Oxford) 2013; 15: 741-746.
2) Czauderna P, Lopezterrada D, Hiyama E, Haberle B, Malogolowkin MH, Meyers RL. Hepatoblastoma state of the art: pathology, genetics, risk stratification, and chemotherapy. Curr Opin Pediatr 2014; 26: 19-28.
3) Meyers RL, Rowland J, Krailo M, Chen Z, Katzenstein HM, Malogolowkin MH. Predictive power of pretreatment prognostic factors in children with hepatoblastoma: a report from the Children's Oncology Group. Pediatr Blood Cancer 2009; 53: 1016-1022.
4) Hooks KB, Audoux J, Fazli H, Lesjean S, Ernault T, Dugotsenant N, Lestelasserre T, Hagedorn M, Rousseau B, Danet C, Branchereau S, Brugières L, Taque S, Guettier C, Fabre M, Rullier A, Buendia MA, Commes T, Grosset CF, Raymond AA. New in-

sights into diagnosis and therapeutic options for proliferative hepatoblastoma. Hepatology 2018; 68: 89-102.

5) Qu S, Yang X, Li X, Wang J, Gao Y, Shang R, Sun W, Dou K, Li H. Circular RNA: a new star of noncoding RNAs. Cancer Lett 2015; 365: 141-148.
6) Hansen TB, Kjems J, Damgaard C. Circular RNA and miR-7 in cancer. Cancer Res 2013; 73: 5609-5612.
7) Chen J, Li Y, Zheng Q, Bao C, He J, Chen B, Lyu D, Zheng B, Xu Y, Long Z, Zhou Y, Zhu H, Wang Y, He X, Shi Y, Huang S. Circular RNA profile identifies circPVT1 as a proliferative factor and prognostic marker in gastric cancer. Cancer Lett 2017; 388: 208-219.
8) Yang Y, Gao X, Zhang M, Yan S, Sun C, Xiao F, Huang N, Yang X, Zhao K, Zhou H, Huang S, Xie B, Zhang N. Novel role of FBXW7 circular RNA in repressing glioma tumorigenesis. J Natl Cancer Inst 2018; 110. doi: 10.1093/jnci/djx166.
9) Jeck WR, Sharpless NE. Detecting and characterizing circular RNAs. Nat Biotechnol 2014; 32: 453-461.
10) Jeck WR, Sorrentino JA, Wang K, Slevin MK, Burd CE, Liu J, Marzluff WF, Sharpless NE. Circular RNAs are abundant, conserved, and associated with ALU repeats. RNA 2013; 19: 141-157.
11) Xuan L, Qu L, Zhou H, Wang P, Yu H, Wu T, Wang X, Li Q, Tian L, Liu M, Sun Y. Circular RNA: a novel biomarker for progressive laryngeal cancer. Am J Transl Res 2016; 8: 932-939.
12) Liu BH, Zhang BB, Liu XQ, Zheng S, Dong KR, Dong R. Expression profiling identifies circular RNA signature in hepatoblastoma. Cell Physiol Biochem 2018; 45: 706-719.
13) Zhang X, Lu W, Zheng Y, Wang W, Bai L, Chen L, Feng Y, Zhang Z, Yuan Z. In situ analysis of intrahepatic virological events in chronic hepatitis B virus infection. J Clin Invest 2016; 126: 1079-1092.
14) Zhou S, Parham DM, Yung E, Pattengale PK, Wang L. Quantification of glypican 3, β-catenin and claudin-1 protein expression in hepatoblastoma and paediatric hepatocellular carcinoma by colour deconvolution. Histopathology 2015; 67: 905-913.
15) Hansen TB, Jensen TI, Clausen BH, Bramsen JB, Finsen B, Damgaard CK, Kjems J. Natural RNA circles function as efficient microRNA sponges. Nature 2013; 495: 384-388.
16) Jang KY, Hwang SH, Kwon KS, Kim KR, Choi HN, Lee N, Kwak J, Park B, Park HS, Chung MJ, Kang MJ, Lee DG, Kim HS, Shim H, Moon WS. SIRT1 expression is associated with poor prognosis of diffuse large B-cell lymphoma. AM J Surg Pathol 2008; 32: 1523-1531.
17) Jang KY, Kim KS, Hwang SH, Kwon KS, Kim KR, Park HS, Park BH, Chung MJ, Kang MJ, Lee DG, Moon WS. Expression and prognostic significance of SIRT1 in ovarian epithelial tumours. Pathology 2009; 41: 366-371.
18) Lee H, Kim KR, Noh SJ, Park HS, Kwon KS, Park B, Jung SH, Youn HJ, Lee BK, Chung MJ, Koh DH, Moon WS, Jang KY. Expression of DBC1 and SIRT1 is associated with poor prognosis for breast carcinoma. Hum Pathol 2011; 42: 204-213.
19) Zhang ZY, Hong D, Nam SH, Kim JM, Paik YH, Joh JW, Kwon CH, Park JB, Choi GS, Jang KY, Park CK, Kim SJ. SIRT1 regulates oncogenesis via a mutant p53-dependent pathway in hepatocellular carcinoma. J Hepatol 2015; 62: 121-130.
20) Bender C, Ullrich A. PRKX, TTBK2 and RSK4 expression causes sunitinib resistance in kidney carcinoma- and melanoma-cell lines. Int J Cancer 2012; 131: E45-E55.
21) Aronson DC, Meyers RL. Malignant tumors of the liver in children. Semin Pediatr Surg 2016; 25: 265-275.
22) Brown J, Perilongo G, Shafford E, Keeling JW, Pritchard J, Brock P, Dicksmireaux C, Phillips A, Vos A, Plaschkes J. Pretreatment prognostic factors for children with hepatoblastoma — results from the International Society of Paediatric Oncology (SIOP) Study SIOPEL 1. Eur J Cancer 2000; 36: 1418-1425.
23) Meyers RL. Tumors of the liver in children. Surg Oncol 2007; 16: 195-203.
24) Maibach R, Roebuck DJ, Brugieres L, Capra M, Brock P, Igna PD, Otte J, De Camargo B, Zsiros J, Zimmermann A, Aronson D, Childs M, Scopinaro M, Morland B, Plaschkes J, Czauderna P, Perilongo G. Prognostic stratification for children with hepatoblastoma: The SIOPEL experience. Eur J Cancer 2012; 48: 1543-1549.
25) Wu JF, Chang HH, Lu MY, Jou ST, Chang KC, Ni YH, Chang MH. Prognostic roles of pathology markers immunoexpression and clinical parameters in Hepatoblastoma. J Biomed Sci 2017; 24: 62.
26) Emre S, Umman V, Rodriguez-Davalos MI. Current concepts in pediatric liver tumors. Pediatr Transplant 2012; 16: 549-563.
27) Qin M, Liu G, Huo X, Tao X, Sun X, Ge Z, Yang J, Fan J, Liu L, Qin W. Hsa_circ_0001649: a circular RNA and potential novel biomarker for hepatocellular carcinoma. Cancer Biomark 2016; 16: 161-169.
28) Chen S, Li T, Zhao Q, Xiao B, Guo J. Using circular RNA hsa_circ_0000190 as a new biomarker in the diagnosis of gastric cancer. Clin Chim Acta 2017; 466: 167-171.
29) Bushati N, Cohen SM. MicroRNA functions. Annu Rev Cell Dev Biol 2007; 23: 175-205.
30) Wang H, Zhi H, Ma D, Li T. MiR-217 promoted the proliferation and invasion of glioblastoma by repressing YWHAG. Cytokine 2017; 92: 93-102.
31) Zhang Q, Yuan Y, Cui J, Xiao T, Jiang D. MiR-217 promotes tumor proliferation in breast cancer via targeting DACH1. J Cancer 2015; 6: 184-191.
32) Zhang M, Li M, Li N, Zhang Z, Liu N, Han X, Liu Q, Liao C. MiR-217 suppresses proliferation, migration, and invasion promoting apoptosis via targeting MTDH in hepatocellular carcinoma. Oncol Rep 2017; 37: 1772-1778.